

A_g Raman modes of RBCO ($R = \text{Gd}, \text{Pr}$) by density functional theory approach

H. Khosroabadi, A. Tavana, and M. Akhavan^a

Magnet Research Laboratory (MRL), Department of Physics, Sharif University of Technology, P.O. Box 11365-9161, Tehran, Iran

Received 18 December 2005 / Received in final form 22 March 2006

Published online 2 June 2006 – © EDP Sciences, Società Italiana di Fisica, Springer-Verlag 2006

Abstract. Ab initio total energy calculations have been performed for superconducting $\text{GdBa}_2\text{Cu}_3\text{O}_7$ and insulating $\text{PrBa}_2\text{Cu}_3\text{O}_7$ using the full-potential linear augmented plane-wave method in the local density approximation (LDA) and generalized gradient approximation (GGA). The comparison of the calculated unit cell volume and lattice parameters with the experimental data indicates the improvement of these parameters in the GGA relative to LDA. LDA and GGA give the equilibrium unit cell volume about 6% smaller and 1.25% larger than the experimental data, respectively for both systems. Thus frozen phonon calculations have been performed to determine the eigenvalues and eigenvectors of the $k = 0$ A_g modes of the two systems in equilibrium structure have been obtained in GGA. The calculated frequencies in the GGA are in good agreement with the other LDA calculations for similar systems. Comparison of computational data with experimental data indicates that calculations determine the frequencies about ten percent below the experimental data. Even by improving LDA to GGA in these calculations, the calculated phonon frequencies have remained almost ten percent below the experimental data, even though the calculated unit cell volumes are nearly equal to the experimental data. So, applying GGA has not considerably decreased the difference between the computational and experimental data. The effect of Pr doping on the eigenvalues and eigenvectors have also been investigated.

PACS. 74.25.Kc Phonons – 31.15.Ew Density-functional theory – 33.20.Fb Raman and Rayleigh spectra (including optical scattering) – 74.72.Bk Y-based cuprates

Introduction

Recent experimental [1,2] and computational [3] studies indicate that the electron-phonon interaction has an important role in the mechanism of superconductivity of high temperature superconductors (HTSCs) while early belief was that the electron-electron interaction being more important [4,5]. Neutron scattering experiments show an appreciable softening of phonon frequency by doping, especially for the oxygen half breathing mode, suggesting a substantial coupling of these modes with the doped holes [6]. Photoemission experiments [1] show a large kink in the hole dispersion at about 70 meV binding energy, suggesting a strong coupling of holes with a bosonic mode with 70 meV energy. A computational study in the $t - J$ model indicates that the strong distance dependence of the hopping and Coulomb integrals results in a strong electron-phonon coupling and explains the softening of half-breathing phonon mode [7]. LDA calculation based on density functional theory indicates the large electron-phonon coupling constant which can produce the high transition temperature in La_2CuO_4 system [8]. On the

other hand, the linear temperature dependence of the resistivity in the wide range of temperature [9] and the small value of isotope coefficient of the optimally doped systems [10] suggest that the electron-phonon plays a secondary role. Some computational studies indicate that the renormalization of electron-phonon interaction by the electronic correlations could explain the anomalous behavior of different transport experiments and introduce a large coupling constant for producing high superconducting transition temperature [11]. Several different research groups are performing more computational and experimental studies to clarify the real participation of the electron-phonon interaction in the mechanism of HTSCs.

The temperature and doping dependences of phonon frequencies give suitable information about the relative degree of electron-phonon coupling in different modes for HTSCs. Two interesting cases for these studies are the oxygen deficiency and Pr substitution which cause the suppression of superconductivity [12]. Pr is an anomaly in the $\text{RBa}_2\text{Cu}_3\text{O}_{7-\delta}$ (RBCO, where R is a rare earth or Y) family of HTSCs that in spite of having orthorhombic crystal structure like other members of this group, behaves as an insulator [13]. In these systems, the Pr

^a e-mail: akhavan@sharif.edu

doping for about 0.3 to 0.6 Pr, depending on the ionic size of R, reduces the transition temperature to zero [14,15]. So, the phonon study of isostructural GdBCO and PrBCO that are superconducting and insulator systems, respectively, could be useful for understanding the anomaly. Raman [16] and neutron scattering [17] measurements on RBCO system indicate that Pr doping changes the phonon frequencies by different values for different modes [18].

Computational studies on the effect of Pr doping on the phonon frequency of HTSC systems have not been considered much. Eigenvalues and eigenvectors of phonon modes have suitable information that could be obtained through these studies. Density functional theory is a conventional approach for calculating the eigenvalues and eigenvectors at least at the center of the Brillouin zone ($k = 0$). Previous calculations indicate that LDA is capable of calculating the structural and vibrational properties of HTSCs, even in the strong correlation regime where the compounds are antiferromagnetic insulator (such as PrBCO) and band structure calculations have shown to have some over-estimations [19].

Previous calculations show that the calculated phonon frequencies in LDA with the experimental unit cell are about ten percent below the experimental values. Frozen phonon calculations in equilibrium unit cell volume, obtained by LDA calculation, indicates that the computational data reaches the experimental ones [19], however, in the experimental unit cell there is ten percent difference yet. In this study, we have calculated the phonon frequencies of GdBCO and PrBCO in GGA, and have compared them with experimental data and computational studies. We will address to the question as how much GGA calculations refine the LDA computational data.

Computational details

The total energy calculations have been performed using ab-initio full potential linear augmented plane waves (FP-LAPW) method based on density functional theory. We have used the Wien2k computational code [20,21] in the LDA and GGA, which is a powerful code in this area, especially for these localized systems. We have used GGA with Perdew-Burke-Ernzerhof parameterization [22]. Due to our interest in calculating the phonon frequencies, not the band structure and density of state, we have not used the LDA+ U approach for the $4f$ states of Gd and Pr ions. Considering constant U for $4f$ orbitals, could correct the band structure and density of state results for $4f$ systems, but makes marginal contribution to the force and total energy calculations. The initial lattice parameters for the calculation have been taken from the experimental data as $a = 3.854 \text{ \AA}$, $b = 3.902 \text{ \AA}$, and $c = 11.676 \text{ \AA}$ for GdBCO, and $a = 3.865 \text{ \AA}$, $b = 3.916 \text{ \AA}$, and $c = 11.688 \text{ \AA}$ for PrBCO [23]. Further, the equilibrium unit cell volume and lattice parameters for the two systems have been derived by Murnaghan fitting of the energy-volume data. The ratios of c/a and b/a have been kept constant for the volume optimization. The initial z ionic positions have been taken from our previous calculation for YBCO [24], and

considered for the two systems as 0.1568, 0.1800, 0.3555, 0.3781, and 0.3790 for O(4), Ba, Cu(2), O(3), and O(2), respectively. By using the computational lattice parameters, to derive the internal positions, ion relaxation has been performed to converge the ionic forces to better than 0.5 mRy/a.u.

The radii of muffin-tin spheres of O, Cu, Ba, Gd, and Pr ions have been considered to be 1.6, 1.8, 2.3, 2.5, and 2.5 a.u., respectively. These values are kept fixed in all of the calculations, and have been chosen such that they remain non-overlapping in the volume optimization and phonon frequency calculation. The energy to separate core and valence states has been set as a default value -6 Ry . The $R_{MT} \times K_{max}$ and cut off angular momentum L_{max} parameters have been considered for these calculations as 7.0 and 10, respectively. Performing the calculation for different number of k points, indicates that the number of k points between 100 and 500 sampling in the First Brillouin zone (corresponding to 9 to 72 k points in the irreducible wedge of the Brillouin zone) is sufficient to calculate the total energy of these systems. We have performed the calculation at 500 k points corresponding to 72 k points in the irreducible wedge of the Brillouin zone. This number of k points is in correspondence with $11 \times 11 \times 3$ mesh in the Monkhorst-Pack scheme. The Broyden factor for these systems that includes Pr, Gd, and Cu ions with localized f and d orbitals has been set to 0.10 to avoid convergence difficulty.

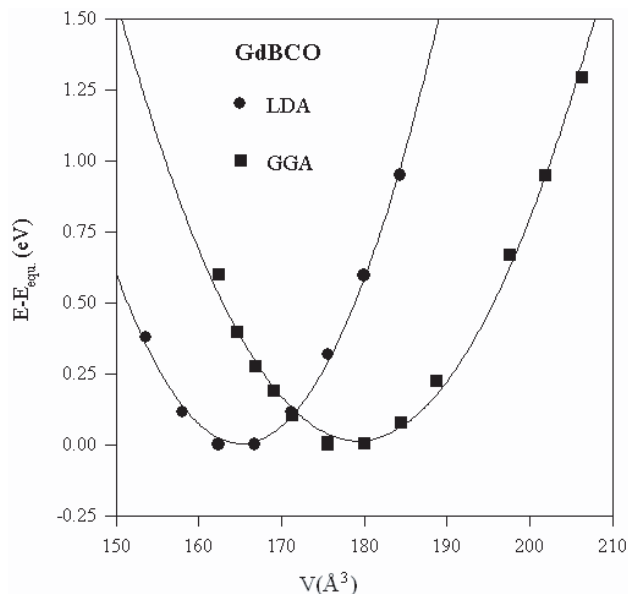
To calculate the frozen phonon frequencies (at $k = 0$) we have displaced one of Ba, Cu(2), O(2), O(3), and O(4) ions in each calculation by step $0.002c$ in the $0.016c$ region around the ionic equilibrium positions, while other ions have been kept in their equilibrium positions. The total energy has converged in each calculation to better than $10^{-4} \text{ Ry}/(\text{unit cell})$.

Results and discussion

To begin with, we have calculated the equilibrium lattice parameters, equilibrium unit cell volume, and bulk modulus from the Murnaghan fitting of total energy-volume curves for the two systems in different LDA and GGA. Figure 1 shows the computational data in the LDA and GGA with their Murnaghan fitting for GdBCO. The corresponding figure for PrBCO is very similar to Figure 1. The equilibrium lattice parameters (with constant c/a and b/a ratio) and volume for the two systems in the GGA are shown in Table 1. The numbers in parentheses indicate the relative percentage difference with the experiment. The corresponding values in the LDA are $a = 3.770 \text{ \AA}$, $b = 3.817 \text{ \AA}$, $c = 11.422 \text{ \AA}$, and $V = 164.38 \text{ \AA}^3$ for GdBCO, and $a = 3.790 \text{ \AA}$, $b = 3.840 \text{ \AA}$, $c = 11.460 \text{ \AA}$, and $V = 166.79 \text{ \AA}^3$ for PrBCO. Comparing these data with experimental data shows that the computational data in the GGA for all of lattice parameters is about 0.41% larger than the experimental data, and for volume it is about 1.22% and 1.28% larger than the experimental values for PrBCO and GdBCO, respectively, while the corresponding values are about -2% for lattice parameters and -5.7%

Table 1. Equilibrium lattice parameters, unit cell volume, bulk modulus, and ionic positions in GGA calculation for GdBCO and PrBCO systems. The numbers in parentheses indicate the relative percentage difference with the experiment.

	a_{eq} (Å)	b_{eq} (Å)	c_{eq} (Å)	V_{eq} (Å ³)	B (GPa)	Z_{Ba}	$Z_{Cu(2)}$	$Z_{O(2)}$	$Z_{O(3)}$	$Z_{O(4)}$
PrBCO	3.881 (+0.41%)	3.932 (+0.41%)	11.735 (+0.40%)	179.08 (+1.22%)	124	0.1743	0.3523	0.3802	0.3809	0.1635
GdBCO	3.870 (+0.42%)	3.919 (+0.44%)	11.725 (+0.42%)	177.82 (+1.28%)	119	0.1790	0.3558	0.3798	0.3799	0.1618

**Fig. 1.** The computational data for energy-volume calculation in LDA and GGA for GdBCO. The lines show the Murnaghan fitting of the calculated data.

to -6.4% for volume in the LDA calculation. These calculations indicate the capability of the Wien2k code in GGA for determining the equilibrium lattice parameters and volume, and their optimization with respect to the LDA calculation. It should be noted that the usual underestimation of equilibrium unit cell volume in the LDA for similar systems is about $3.5\text{--}6\%$ [19, 24]. The effect of volume optimization on phonon frequencies will be discussed in the following.

The relative z coordination of equilibrium ionic positions of O(4), Ba, Cu(2), O(3), and O(2) ions have been derived from ionic relaxation and inserted in Table 1. These data are in good agreement with experimental data [25]. The uncertainties of these values are smaller than 2×10^{-4} , which could be derived from our force calculations. Bulk modulus has been derived to be 157 GPa and 119 GPa for GdBCO, and 151 GPa and 124 GPa for PrBCO in the LDA and GGA, respectively. The values obtained for GGA calculation relative to LDA calculation are in better agreement with the reported data for similar systems [24, 26].

For determining the phonon eigenvalue and eigenvector of A_g Raman modes, we have calculated the dynamical K matrix for Ba, Cu(2), O(2), O(3), and O(4) ions which are active in these Raman modes. Tables 2 and 3 show

Table 2. The elements of dynamical K matrix (eV/Å²) obtained from energy and force fitting for GdBCO system.

	Ba	Cu(2)	O(2)	O(3)	O(4)
Ba	6.40	-0.81	-0.13	-0.19	-0.78
Cu(2)	-0.81	3.67	-1.47	-1.47	1.19
O(2)	-0.13	-1.47	6.63	1.30	-1.00
O(3)	-0.19	-1.47	1.30	7.00	-1.05
O(4)	-0.78	1.19	-1.00	-1.05	10.94

Table 3. The elements of dynamical K matrix (eV/Å²) obtained from energy and force fitting for PrBCO system.

	Ba	Cu(2)	O(2)	O(3)	O(4)
Ba	6.38	-0.57	-0.11	-0.11	-1.05
Cu(2)	-0.57	3.71	-0.90	-0.75	0.47
O(2)	-0.11	-0.90	6.60	1.43	-1.07
O(3)	-0.11	-0.75	1.43	7.94	-1.02
O(4)	-1.05	0.47	-1.07	-1.02	10.09

the elements of the dynamical K matrix for GdBCO and PrBCO, respectively. The diagonal elements have been derived from fitting of the energy position curves for different ionic displacements, while the off diagonal elements have been derived from fitting of the ionic forces versus another ionic displacement, i.e. using the $F_j = K_{ij}z_i$ relation.

From the diagonal elements, we have calculated the bare phonon frequencies as 112, 125, 335, 344, and 430 cm^{-1} for GdBCO, and 112, 126, 334, 366, and 413 cm^{-1} for PrBCO, respectively for Ba, Cu(2), O(2), O(3), and O(4) displacements. We have diagonalized the K matrix to obtain eigenvalues and eigenvectors of A_g Raman modes in these systems. The results are shown in Tables 4 and 5 for GdBCO and PrBCO, respectively. Off diagonal elements decrease Ba and O(2) bare frequencies and increase O(3) and O(4) bare frequencies.

It can be seen from Tables 4 and 5 that the Ba and Cu(2) ions in the first two modes, known as Ba and Cu(2) modes, are considerably mixed, while there is low mixing of these ions with oxygen ions. Also, vibrational amplitudes of Ba and Cu(2) ions are small in the three modes of oxygen ions. This indicates that the Ba and Cu(2) ions in the A_g modes of these systems are decoupled from the oxygen ions. The Ba and Cu(2) ions vibrate in the same phase for the Ba mode, while they are in opposite phases in the Cu(2) mode for the two systems. The vibrational amplitude of Cu(2) ion is larger than Ba ion for the Ba mode in GdBCO, while for PrBCO it is the reverse, as expected. Comparison of the K matrices for GdBCO and PrBCO

Table 4. The eigenvalues and eigenvectors of the A_g Raman active modes of GdBCO system.

A_g mode	Freq. (cm^{-1})	Eigenvectors				
		Ba	Cu(2)	O(2)	O(3)	O(4)
Ba	102	0.58	0.78	0.17	0.16	-0.01
Cu(2)	122	-0.52	0.82	0.15	0.13	-0.11
O(2)-O(3)	305	0.00	-0.01	0.76	-0.65	0.02
O(2)+O(3)	358	-0.01	-0.05	0.59	0.70	0.41
O(4)	444	-0.01	0.05	-0.27	-0.30	0.91

Table 5. The eigenvalues and eigenvectors of the A_g Raman active modes of PrBCO system.

A_g mode	Freq. (cm^{-1})	Eigenvectors				
		Ba	Cu(2)	O(2)	O(3)	O(4)
Ba	107	0.81	0.57	0.10	0.07	0.08
Cu(2)	125	-0.31	0.94	0.11	0.07	-0.06
O(2)-O(3)	309	0.00	-0.02	0.86	-0.50	0.09
O(2)+O(3)	366	-0.01	-0.02	0.38	0.75	0.54
O(4)	432	-0.01	0.02	-0.34	-0.43	0.83

Table 6. The eigenvalues for GdBCO and PrBCO in comparison with the reported computational and experimental data.

Freq. (cm^{-1})	This study		Experimental data		Computational data
	GdBCO	PrBCO	YBCO [27-30]	PrBCO [18,35,36]	YBCO [19,31,32]
A_g mode					
Ba	102	107	110 116-119	115 128 126	95 123 102 103
Cu(2)	122	125	150 145-159	150 149 150	130 147 127 130
O(2)-O(3)	305	309	330 335-336	306 298 —	330 338 317 327
O(2)+O(3)	358	366	440 435-440	442 430 440	400 422 387 387
O(4)	444	432	500 493-500	529 516 524	460 487 450 452

shows that the largest differences of their elements are $K_{\text{Ba}-\text{Cu}(2)}$, $K_{\text{Cu}(2)-\text{O}(2)}$, $K_{\text{Cu}(2)-\text{O}(3)}$, and $K_{\text{Cu}(2)-\text{O}(4)}$. From changing these elements, it is concluded that the eigenvectors of Ba and Cu(2) modes are not very sensitive to the $K_{\text{Ba}-\text{Cu}(2)}$ and $K_{\text{Cu}(2)-\text{O}(4)}$ elements, while they are sensitive to the $K_{\text{Cu}(2)-\text{O}(2)}$ and $K_{\text{Cu}(2)-\text{O}(3)}$ elements. Reducing the $K_{\text{Cu}(2)-\text{O}(2)}$ and $K_{\text{Cu}(2)-\text{O}(3)}$ of the GdBCO K matrix to the one for PrBCO, results in the increase of the vibrational frequency of Ba ion relative to the Cu(2) ion in Ba mode. In the O(2)-O(3) mode of these systems O(2) and O(3) ions are in opposite phases, and are decoupled from other ions, while for the O(2)+O(3) mode, O(2) and O(3) ions are in the same phase and couple with the O(4) ion in the same phase. The results are in agreement with other computational studies [19].

Table 6 shows the eigenvalues of different modes against other experimental [27-30] and computational [19,31,32] data for similar systems. Comparison of the data shows that the calculated data are in the range of computational error for these calculations, which is about ten percent. Previous studies in this field indicate that the local density calculated phonon frequencies in the experimental lattice parameters are about ten percent lower than the Raman data. A very accurate study in the calculation of these eigenvalues indicates that by reducing the experimental lattice parameters to the theoretical equilibrium values, even in the local density approximation, all five modes are significantly enhanced and the average

discrepancy between the experimental and computational data are reduced to zero [19].

In this study, we have optimized the volume in the GGA, and found the computational equilibrium volume to be 1.22% and 1.28% larger than the experimental value for PrBCO and GdBCO systems, respectively. This is a noticeable point, because previous studies have obtained a value of about 6% underestimation of the volume in their computational optimization [19]. So, phonon frequency calculations in the optimized volume in GGA of our study increase a little the difference between the experimental and computational studies. This study indicates that the computational phonon frequencies in equilibrium unit cell volume, which is about 6% below the experimental value in LDA, reaches the experimental data. So, if the volume optimization with some correction to the LDA, such as GGA, is obtained near the experimental value, the phonon frequencies have an underestimation of about ten percent. It is resulted that doing calculations in the GGA could not refine the ten percent difference between the experimental and computational data.

This calculation indicates that A_g frequencies do not change considerably after substitution of Gd by Pr ion, and the small differences (highest change is 11 cm^{-1} for O(4) mode), as shown in Table 6, are within the computational uncertainty (about 2%). Calculations show that the eigenvalue for the O(4) mode has been decreased by Pr doping, while other frequencies have been increased with

Pr doping. Increasing the K elements for O(2) and O(3), and frequencies of O(2)+O(3) and O(2)–O(3) modes by Pr doping could indicate the increase of the strength of Pr–O(2) and Pr–O(3) bonds. This could be an evidence for strong hybridization of Pr with O(2) and O(3), which causes localization of holes in the CuO_2 planes in the Fehrenbacher and Rice (FR) model [33]. More recently, Liechtenstein and Mazin have confirmed and also improved the FR model by computing more exactly the role of Pr in suppression of superconductivity in RPrBCO [34]. Some experimental data, however, show that by Pr substitution, the O(4) mode hardens while the O(2)–O(3) modes softens [18, 35, 36].

Conclusions

We have calculated the eigenvalues and eigenvectors of A_g modes of two isostructural superconducting GdBCO and insulating PrBCO based on density functional theory. Volume optimization in LDA has resulted that while these values are about 6% lower than the experimental data, GGA improves this to about 1.25% larger than the experimental data. In this situation, i.e. when we use the equilibrium unit cell volume obtained in GGA calculation, the computational frequencies are about ten percent below the experimental values. Our results indicate that the performed GGA calculation does not refine this underestimation. When the equilibrium unit cell volume reaches the experimental value, the computational eigenvalues go below the experimental values. Substitution of Pr for Gd in GdBCO system does not change the eigenvalues and eigenvectors of GdBCO, and their differences are within the computational underestimation.

Fruitful discussions with C. Ambrosch-Draxl is acknowledged. This work was supported in part by the Offices of the Vice President for Research and the Dean of Graduate Studies at Sharif University of Technology.

References

1. A. Lanzara, P.V. Bogdanov, X.J. Zhou, S.A. Kellar, D.L. Feng, E.D. Lu, T. Yoshida, H. Eisaki, A. Fujimori, K. Kishio, J.-I. Shimoyama, T. Noda, S. Uchida, Z. Hussain, Z.-X. Shen, *Nature* **412**, 510 (2001)
2. G.-H. Gweon, T. Sasagawa, S.Y. Zhou, J. Graft, H. Takagi, D.-H. Lee, A. Lanzara, *Nature* **430**, 187 (2004)
3. M.L. Kubic, O.V. Dolgov, *Phys. Rev. B* **71**, 092505 (2005)
4. P.W. Anderson, *Science* **235**, 1196 (1987)
5. P. Monthoux, A.V. Balatsky, D. Pines, *Phys. Rev. B* **46**, 14803 (1992)
6. <http://www.fkf.mpg.de/andersen/phonons/hightc.html>
7. O. Rosch, O. Gunnarsson, *Phys. Rev. Lett.* **92**, 146403 (2004)
8. H. Krakauer, W.E. Pickett, R.E. Cohen, *Phys. Rev. B* **47**, 1002 (1993)
9. P.B. Allen, in *Physical Properties of High Temperature Superconductors*, edited by D.M. Ginsberg (World Scientific, Singapore, 1989), Vol. I, p. 213
10. J.P. Franck, in *Physical Properties of High Temperature Superconductors*, edited by D.M. Ginsberg (World Scientific, Singapore, 1994), Vol. IV, p. 189
11. M.L. Kubic, *Phys. Rep.* **338**, 1 (2000)
12. H. Khosroabadi, V. Daadmehr, M. Akhavan, *Mod. Phys. Lett. B* **16**, 943 (2002)
13. H. Khosroabadi, M. Modarreszadeh, P. Taheri, M. Akhavan, *J. Superconductivity* **17**, 749 (2003)
14. M. Akhavan, *Physica B* **321**, 265 (2002)
15. Y. Xu, W. Guan, *Phys. Rev. B* **45**, R3176 (1992)
16. R. Bhadra, T.O. Brun, M.A. Beno, B. Dabrowski, D.G. Hinks, J.Z. Liu, J.D. Jorgensen, L.J. Nowicki, A.P. Paulikas, I.K. Schuller, C.U. Segre, L. Soderholm, B. Veal, H.H. Wang, J.M. Williams, K. Zhang, M. Grimsditch, *Phys. Rev. B* **37**, 5142 (1988)
17. C.H. Gardiner, A.T. Boothroyd, B.H. Larsen, W. Reichardt, A.A. Zhokhov, N.H. Andersen, S.J.S. Lister, A.R. Wildes, e-print [arXiv:cond-mat/0310555](https://arxiv.org/abs/cond-mat/0310555)
18. A.P. Litvinchuk, C. Thomsen, I.E. Trofimov, H.-U. Habermeier, M. Cardona, *Phys. Rev. B* **46**, 14017 (1992)
19. R. Kouba, C. Ambrosch-Draxl, B. Zangger, *Phys. Rev. B* **60**, 9321 (1999)
20. P. Blaha, K. Schwarz, G.K.H. Madsen, D. Kvasnicka, J. Luitz, *Wien2k, An Augmented Plane Wave + Local Orbitals Program for Calculating Crystal Properties* (Karlheniz Schwarz, Techn. Universitat Wien, Austria, 2001)
21. P. Blaha, K. Schwarz, P. Sorantin, B. Trickey, *Comput. Phys. Commun.* **59**, 399 (1990)
22. J.P. Perdew, K. Burke, M. Ernzerhof, *Phys. Rev. Lett.* **77**, 3865 (1996)
23. Z. Yamani, M. Akhavan, *Physica C* **268**, 78 (1996)
24. H. Khosroabadi, B. Mossalla, M. Akhavan, *Phys. Rev. B* **70**, 134509 (2004)
25. R.M. Hazen, in *Physical Properties of High Temperature Superconductors*, edited by D.M. Ginsberg (World Scientific, Singapore, 1989), Vol. II, p. 121
26. X.J. Chen, C.D. Gong, Y.B. Yu, *Phys. Rev. B* **61**, 3691 (2000)
27. *Physical Properties of High Temperature Superconductors*, edited by C. Thomsen, M. Cardona, D.M. Ginsberg (World Scientific, Singapore, 1989), Vol. I, p. 409
28. T. Strach, T. Ruf, E. Schönherr, M. Cardona, *Phys. Rev. B* **51**, 16460 (1995)
29. G. Burns, F.H. Dacol, F. Holtzberg, D.L. Kaiser, *Solid State Commun.* **66**, 217 (1988)
30. K.F. McCarty, J.Z. Liu, R.N. Shelton, H.B. Radousky, *Phys. Rev. B* **41**, 8792 (1990)
31. C.O. Rodriguez, A.I. Liechtenstein, I.I. Mazin, O. Jepsen, O.K. Andersen, M. Methfessel, *Phys. Rev. B* **42**, R2692 (1990)
32. C. Ambrosch-Draxl, R. Kouba, P. Knoll, *Z. Phys. B* **104**, 687 (1997)
33. R. Fehrenbacher, T.M. Rice, *Phys. Rev. Lett.* **70**, 3471 (1993)
34. A.I. Liechtenstein, I.I. Mazin, *Phys. Rev. Lett.* **74**, 1000 (1995); I.I. Mazin, A.I. Liechtenstein, *Phys. Rev. B* **57**, 150 (1998)
35. H.B. Radousky, K.F. McCarty, J.L. Peng, R.N. Shelton, *Phys. Rev. B* **39**, R12383 (1999)
36. I.-S. Yang, G. Burns, F.H. Dacol, C.C. Tsuei, *Phys. Rev. B* **42**, 4240 (1990)